ARTICLES

Diastereoselective Self-Assemblies of Chlorophylls *a* and *a*′

Hiroyasu Furukawa,† Toru Oba,*,‡,§ Hitoshi Tamiaki,‡ and Tadashi Watanabe*,†

Institute of Industrial Science, University of Tokyo, Roppongi, Minato-ku, Tokyo 106-8558, Japan, and Department of Bioscience and Biotechnology, Ritsumeikan University, Kusatsu, Shiga 525-8577, Japan

Received: January 6, 1999; In Final Form: May 3, 1999

The aggregation behaviors of mixtures of chlorophylls (Chl) *a* and *a*′, the C13^2-(R) and -(S) epimers, were examined in 2-propanol/water = 26/74 (v/v). In the aggregated states, the epimeric mixtures of Chl *a*/*a*′ at molar ratios ranging from 70:30 to 30:70 gave two distinct Q_y absorption bands (at ca. 700 and 750 nm) characteristic of the aggregate colloid of each epimer. On the other hand, a single 750 nm (700 nm) band was observed in the range of the epimeric composition ranges outside the one mentioned above. The time course of the aggregation, disaggregation behavior, filtrations of the colloidal solutions combined with dynamic light-scattering measurements, and fluorescence, resonance Raman, and circular dichroism spectroscopies demonstrated the coexistence of two types of aggregate structures in each colloidal particle. This is the first report suggesting that an epimer pair of chlorophyllous pigments self-assembles simultaneously through limited diastereoselective separation. The phenomenon was rationalized in terms of the phase separation of a regular solution. The diastereocontrol in the self-assembly of other type Chl diastereomers, bacteriochlorophylls *c*, *d*, and *e* possessing chirality at the C3^1-position, was also discussed in relation to supramolecular structures of the self-aggregates in antenna of green photosynthetic bacteria.

Introduction

It is of general interest that a chirality of a single molecule can be amplified in supramolecular structures through self-assembly.[1−6] Upon the formation of supramolecules bearing some structural disorder, such as gels or liquid crystals of biofunctional molecules and synthetic amphiphiles; however, even epimeric pairs of diastereomers do not necessarily self-assemble through spontaneous chiral resolution. Studies on this uncertainty may not only contribute to the development of advanced materials such as ferroelectric liquid crystals but provide an insight into the effects of chirality in living organisms.

Chlorophylls (Chls) are pigments whose stereochemistry has been discussed in relation to the regulation of the structures and functions of their associated forms in vivo.[7−12] Green photosynthetic bacteria have unique light-harvesting apparatus called chlorosomes. The functional core of a chlorosome consists of the self-aggregates of bacteriochlorophylls (BChl) *c*, *d*, and *e* (Figure 1).[7−9] These Chls possess an asymmetric carbon atom at the C3^1 position, and both R and S epimers are found in the organisms: an epimeric ratio of R/S = 2:1 was found for *Chloroflexus aurantiacus*,[13] while there were various ratios for *Chlorobiaceaes*.[14−16] Though the coexistence of the epimeric pair may tune the antenna function of the organisms to a particular ecological niche, it is uncertain whether these epimers in vivo form their own aggregates stereoselectively or randomly mixed aggregates. To date, there have been a limited number of reports on the influence of the C3^1 chirality on the Chl self-assemblies.[17−22] Each epimer showed different aggregation behaviors in nonpolar solvents: the C3^1-(S) epimers tended to leave monomer molecules much more than the C3^1-(R) epimers, and the Q_y absorption maxima of the R and S aggregates differed by 2−47 nm. However, these aggregations must have yielded several oligomeric species which gave several spectral components and broadened absorption spectra; such a heterogeneity makes it difficult to determine whether the R and S epimers self-assemble separately from an epimeric mixture, even though

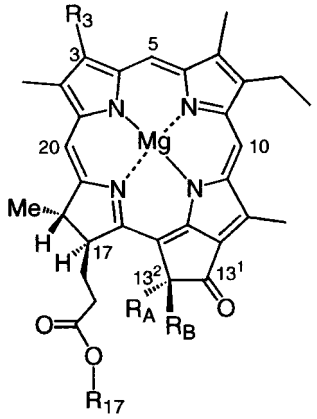

Figure 1. Molecular structure of Chl *a*, Chl *a*′, and BChl *d* (one of chlorosomal Chls) with partial numbering according to the IUPAC system. Chl *a*, R_A = $COOCH_3$, R_B = H, R_3 = CH=CH_2, R_{17} = phytyl; Chl *a*′, R_A = H, R_B = $COOCH_3$, R_3 = CH=CH_2, R_{17} = phytyl; BChl *d*, R_A = R_B = H, R_3 = CH(OH)CH_3, R_{17} = farnesyl, etc.

* Corresponding authors.
† University of Tokyo.
‡ Ritsumeikan University.
§ Present address: Department of Applied Chemistry, Faculty of Engineering, Utsunomiya University, Utsunomiya, Tochigi 321-8585, Japan. Phone: +81-28-689-6158. Fax: +81-28-689-6009. E-mail: obat@cc.utsunomiya-u.ac.jp.

10.1021/jp990079y CCC: $18.00
Published on Web 08/12/1999

there is a large difference between the Q_y absorption maxima of the epimerically pure aggregates. This attempt may also be hampered by much faster intermolecular *random* associations of epimeric Chls than the possible chiral selection under the conditions of these in vitro aggregations in nonpolar solvents.

There exists another epimer pair of chlorophyllous pigments whose stereochemistry in vivo is a matter of argument. Chl *a*′, the $C13^2$-(S) epimer of Chl *a* (Figure 1), was found in the core part of the reaction center complex of photosystem I of oxygen-evolving organisms,[10,11] and the aggregation behavior of this exotic pigment was examined in relation to its possible function in vivo.[12,23−25] Chl *a*′ in aqueous alcohols gives a single aggregate species of a characteristic Q_y absorption around 700 nm, and the Chl *a* aggregate shows a single, broad Q_y band at ca. 750 nm.[12,24,25] Recently we revealed that the Chl *a*′ aggregate colloid clearly distinguishes its supramolecular structure from that of the Chl *a* aggregate by the molecular arrangements as well as the degree of hydration.[25] The different molecular arrangements and the set of sharp, well-resolved marker absorption (Q_y) bands of the epimers suggest that it is possible to clarify whether Chls *a* and *a*′ form their own self-aggregates spontaneously at the same time from an appropriate epimeric mixture. The aggregation behavior of the Chl *a*/*a*′ mixture can be a reference in considering the diastereocontrol in the self-assembly of chlorosomal Chls. However, previous studies do not necessarily support the simultaneous formations of the separate aggregates of Chl *a* and *a*′. Hynninen and Lötjönen reported that Chl *a* readily precipitated upon washing a Chl *a*/*a*′ mixture in light petroleum with water, while no Chl *a*′ precipitated unless the solution was concentrated and cooled (60% de);[26] this confirms a difference in the solubilities alone. Watanabe et al. reported that the aggregate absorption spectrum of the Chl *a*/*a*′ mixture formed in methanol/water = 60:40 was not interpreted as a simple sum of those of pure Chl *a* and *a*′: a bell-shape absorption at 700−720 nm for Chl *a*/*a*′ = 1:0−2:1; a broad absorption at ca. 725 nm with a minor peak at ca. 670 nm for Chl *a*/*a*′ = 2:1−1:2; a doublet peaking at 692 and 713 nm for Chl *a*/*a*′ = 1:2−0:1.[23]

Here, we report the first evidence that the epimeric pair of chlorophyllous pigments, Chl *a* and *a*′, diastereoselectively self-assembled at the same time in 2-propanol/water = 26:74 (v/v; 2P 26% for brevity) where fairly stable aggregates were obtained.[25] Visible absorption, fluorescence, resonance Raman (RR), and circular dichroism (CD) spectroscopies and dynamic light-scattering (DLS) techniques revealed the coexistence of two types of aggregate structures in each colloidal particle. The phenomenon is rationalized in terms of the phase separation of a regular solution and is discussed in relation to the diastereo-controlled aggregations of the chlorosomal Chls.

Materials and Methods

Materials. The preparation of pure Chl *a* and *a*′ was described elsewhere.[12,27] Chl *a* was extracted from lyophilized spinach leaf tissues and was purified using a preparative normal-phase HPLC (column: Senshupak Silica-5251N, 20 mm diameter × 250 mm, 4 °C; eluent: 100:0.8:0.4 hexane/2-propanol/methanol). Chl *a*′ was obtained by partial epimerization of Chl *a* followed by HPLC purification. Pigment mixtures of prescribed epimeric composition were stored in 5 mL glass vials in a solid form at −30 °C until use (total 50 nmol, pigment purity > 99%). The integrity of the pigment during the experiments was ensured by analytical silica HPLC (column: Senshupak Silica-1251N 4.6 mm diameter × 250 mm, 4 °C; eluent: 100:0.8:0.4 hexane/2-propanol/methanol).[28] HPLC grade hexane, methanol, and 2-propanol and reagent grade chloroform and acetone (Wako) were used without further purification. Water was purified with a Milli-Q system (Millipore, Ltd.).

Preparation and Spectroscopy of Chl *a*/*a*′ Aggregates. In what follows, the epimeric composition is denoted by the mole fraction of Chl *a* (x_A) in the epimeric mixture. The pigments were dissolved with 2-propanol (1.3 mL) in the vial, and the solution was diluted quickly with water (3.7 mL) followed by stirring for 3 min.[12,24,25] This colloidal solution (nearly 10 μM on a total monomer basis concentration) was incubated for about 20 h at 20−25 °C in the dark. Visible absorption spectra of the aggregate solutions were recorded on a JASCO spectrophotometer V-560. CD and fluorescence measurements were performed on a JASCO spectropolarimeter J-720W and a Hitachi fluorescence spectrophotometer F-3500, respectively. RR spectra were obtained on a Jobin−Yvon Raman system T 64000 with 4 cm^{-1} resolution. The total concentration of the sample solution for the RR measurements was 50 μM, prepared as described above, and was irradiated with a 457.9 nm line of an Ar^+ laser (NEC GLG-3460, ∼20 mW).

Hydrodynamic diameters of the aggregate colloids were measured using a light-scattering spectrometer DLS-700 (Otsuka Electronics) with the photomultiplier set at a scattering angle of 90°. The sample with a total concentration of 10 μM was irradiated with a 5 mW He−Ne laser at 25 °C. The data obtained were analyzed on an NEC PC-9801 DA with a packaged software.

An aggregate solution (10 μM, $x_A = 0.49$) was filtrated with suction (20 Torr) using the following filters of different pore sizes: filter A, pore size = 700 nm (Fuji Film FR-70, cellulose); filter B, pore size = 400 nm (Fuji Film FR-40, cellulose); filter C, pore size = 200 nm (Millipore JGWP, poly(tetrafluoroethylene)). Absorption spectra of colloidal fractions of different particle sizes were obtained by the subtractions between the spectra of the filtrates. Chls in the filtrate were extracted with chloroform and were subjected to the HPLC analysis stated above to determine the epimeric composition.

Results

Epimeric Composition Dependence of Visible Absorption Spectra. Figure 2 illustrates the epimeric composition dependence of visible absorption spectra of Chl *a*/*a*′ mixtures in 2P 26% (2-propanol/water = 26:74, v/v) recorded at stationary states. The spectrum of pure Chl *a* ($x_A = 1$, top in Figure 2) shows a Q_y absorption band at 747 nm and a Soret maximum at 451 nm.[25] The Q_y band is much more intense than the Soret peak. On the other hand, pure Chl *a*′ ($x_A = 0$, bottom in Figure 2) gives a Q_y band at 698 nm and a Soret peak at 441 nm, and the intensities of the two bands are roughly the same. The red shifts of these Q_y absorption bands from the corresponding monomeric peak (666 nm in 2-propanol) indicate that the Chls were in the self-assembled states.[12,24,25] The 698 and 747 nm absorptions were attributable to the aggregates of ordered molecular arrangements.[25] Prolonged incubation of the 698 nm absorbing Chl *a*′ aggregate solution did not yield the 747 nm absorbing species. DLS measurements revealed that these aggregate species were in the colloidal dimension (average hydrodynamic diameters: Chl *a*, ca. 500 nm; Chl *a*′, ca. 120 nm).[24] No degradation of the pigments including epimerization occurred during the aggregation, as confirmed by HPLC analyses.[27,28] The above set of sharp Q_y bands separated by ca. 50 nm, given in this particular medium, facilitated the observation of the postulated diastereoselective phenomenon.

The absorption spectrum shows systematic transformation with a decrease of x_A from 1 to 0 (Figure 2). The 747 nm band

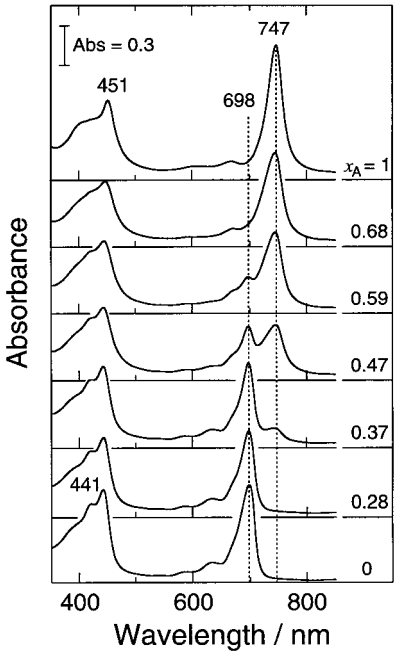

Figure 2. Epimeric composition dependence of the visible absorption spectrum of Chl *a*/*a*′ mixed aggregates recorded at stationary states. Solvent, 2P 26% (2-propanol/water = 26:74); total pigment concentration, 10 μM on monomer basis; temperature, 25 °C. With a decrease of x_A from 1 to 0, the 698 nm band increases while the 745 nm one decreases.

is a single Q_y absorption over the range $x_A = 1-0.7$, with slight blue shift and broadening. In the range x_A = ca. 0.7−0.3, the 747 nm absorption decreases in pace with an increase of the 698 nm band. A roughly equimolar epimeric mixture clearly gives two Q_y bands at 745 and 698 nm with comparable peak heights. It is noted that the spectral shape at $x_A = 0.47$ is nearly the same as that for the equimolar mixture of the stationary aggregates of pure Chl *a* and *a*′ (data not shown). The solutions below ca. 0.3 of x_A give only one Q_y band again, and retain the Q_y peak at 698 nm. A small shoulder component at around 670 nm indicates the presence of the residual precursor, amorphous aggregate (see below and ref 12 and 24). Because the positions of the Q_y peaks (∼745 and ∼698 nm) are nearly independent of the epimeric composition, it is suggested that two types of aggregate structures characteristic of pure Chl *a* and *a*′ coexisted in the range of $x_A = 0.7-0.3$. Above $x_A = 0.7$ and below $x_A = 0.3$, on the other hand, the formed aggregate structure may reflect that of the major epimer.

Fluorescence Spectra. Parts a and b of Figure 3 show the fluorescence emission and excitation spectra of the aggregate formed at an epimeric composition of $x_A = 0.55$. This Chl *a*/*a*′ mixed aggregate gives a dominant fluorescence emission band at 750 nm with a very small shoulder at around 700 nm (excited at 442 nm; solid curve in Figure 3a). These band positions are characteristic of the pure Chl *a* and *a*′ aggregates, though the intensities of these bands are quite different from those of an equimolar mixture of the Chl *a* aggregate and the Chl *a*′ aggregate (excited at 439 nm; broken curve in Figure 3a). The excitation spectrum of the epimeric mixture aggregate (monitored at 800 nm; solid curve in Figure 3b) gives a single spectral component with its maximum at 730−740 nm corresponding to the 746 nm absorption band (broken curve in Figure 3b).[29] It is noted that there is no peak at around 698 nm in the excitation spectrum. This clearly demonstrates that the 698 and 745 nm absorption bands originate from two different aggregate

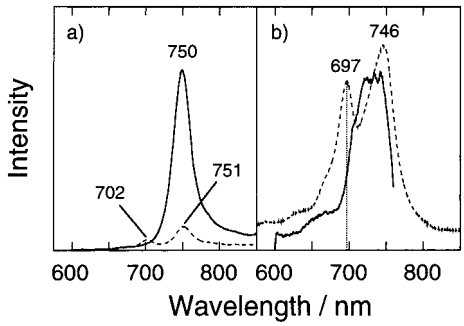

Figure 3. (a) Fluorescence emission spectra (solid curve, λ_{ex} = 442 nm) of Chl *a*/*a*′ mixed aggregate ($x_A = 0.55$, 2P 26%, 10 μM on monomer basis, 25 °C). Dotted curve shows a fluorescence spectrum of an equimolar mixture of the stationary Chl *a* ($x_A = 1$) and *a*′ ($x_A = 0$) aggregates (total pigment concentration, 10 μM on monomer basis; λ_{ex} = 439 nm). (b) Fluorescence excitation spectrum of this epimeric mixture aggregate (λ_{em} = 800 nm). Dotted curve represents the absorption spectrum of this aggregate.

structures. Essentially the same results were obtained for the other epimeric mixtures at around $x_A = 0.5$ (data not shown).

Time Course of the Aggregation. Figure 4a shows the time course of the transformation of the absorption spectrum during the aggregation ($x_A = 0.47$). At the instant of water admixing to the 2-propanol solution of Chls, amorphous aggregates whose broad Q_y absorption peaked at 672 nm and tailed to the longer wavelength region was abruptly formed.[12,24] During the incubation of the solution at 25 °C for ca. 20 h, new absorption bands developed in the wavelength region longer than 700 nm at the expense of the broad 672 nm absorption.[12] The 698 nm band increased more rapidly than the 745 nm band, and the former reached its maximum intensity 3−4 h from the start of the aggregation. The 745 nm band grew up slowly with a small decrease of the 698 nm band during an additional 17 h of incubation. Finally, the system reached a stationary state (>20 h) where these two Q_y bands showed comparable intensities. The temporal changes of the absorbances at 745 and 672 nm drew sigmoid curves (Figure 4b).[12]

The aggregation was also monitored by DLS ($x_A = 0.49$). The time course of the development of the most abundant fraction in the size distribution is shown in Figure 4c. The amorphous aggregate colloid had a hydrodynamic diameter of ca. 50 nm.[24] The particle size grew up rapidly in the early aggregation stage and reached the maximum size of ca. 210 nm at 5 h from the start of the aggregation. Thus, the formed polydisperse colloidal system kept the particle size unchanged even during an additional 20 h of incubation. These time courses suggest that the aggregates of the ordered structures developed through collision and coalescence of the colloidal particles.

Disaggregation Behavior. Dilution of the stationary aggregate solution with acetone induced disaggregation to yield monomeric dispersion. Figure 5 shows the absorption spectral transformation during the titration of an aggregate solution at $x_A = 0.55$ (with intensities corrected for the volume). No change was noted up to 0.05 mL of acetone to 1 mL of aggregate solution. With the addition of 0.1−0.35 mL acetone, the 698 nm band nearly exclusively reduced its intensity, while the 745 nm band decreased only minimally. The epimeric composition of the released monomers at this stage was Chl *a*/*a*′ = 30:70 ($x_A = 0.3$), demonstrated by HPLC analysis after filtration of the aggregate solution; no 745 nm band but the monomeric Q_y band at 666 nm was observed for the filtrate. Further addition of 0.4 mL acetone decreased the broad 745 nm component. All the aggregates were finally converted into monomers with the

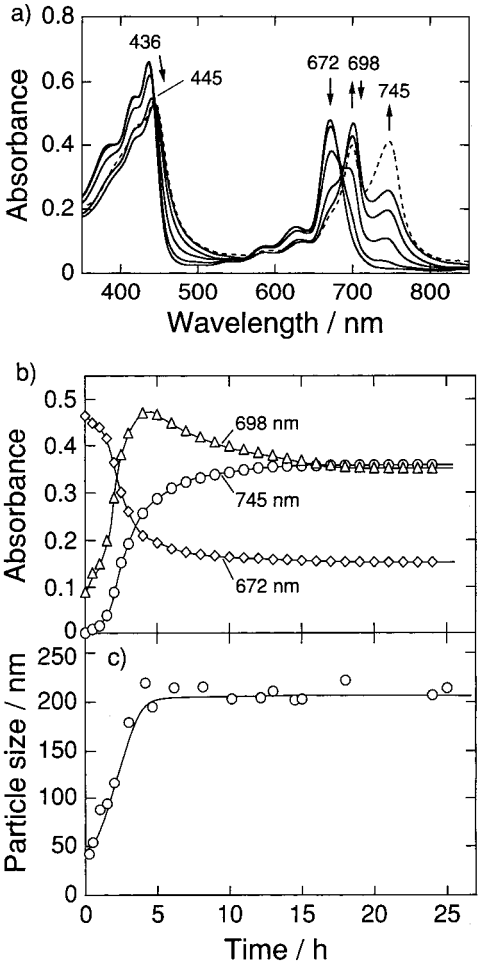

Figure 4. (a) Time course of the absorption spectrum of Chl *a*/*a*′ mixed aggregate solution ($x_A = 0.47$, 2P 26%, 10 μM on monomer basis, 25 °C). Solid curves: 0, 50, 100, 150, and 200 min after preparation of the aggregates. Broken curve: stationary state (>20 h). (b) The development of absorbances at characteristic wavelength positions in Figure 4a. Square, 672 nm; triangle, 698 nm; circle, 745 nm. (c) Time course of the development of the hydrodynamic diameter (most abundant fraction in the size distribution) of the aggregate colloid monitored by DLS ($x_A = 0.49$, 2P 26%, 10 μM on monomer basis, 25 °C).

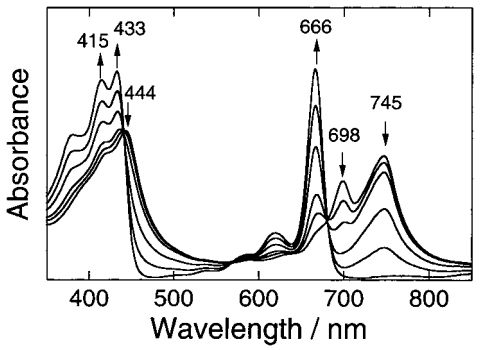

Figure 5. Disaggregation behavior of Chl *a*/*a*′ mixed aggregate solution ($x_A = 0.55$, 1 mL) by dilution with acetone. Acetone added was 0, 0.2, 0.3, 0.4, 0.45, 0.55 mL, respectively. The spectral intensities were corrected for the volume. The original aggregate solution was obtained under the same conditions as in Figure 2 (2P 26%, 10 μM on monomer basis, 25 °C).

admixing of 0.55 mL of acetone. This behavior strongly suggests that the 698 and 745 nm bands originated from different aggregate structures in which each epimer was concentrated.

Filtration of the Aggregate Solution. There was a trend that

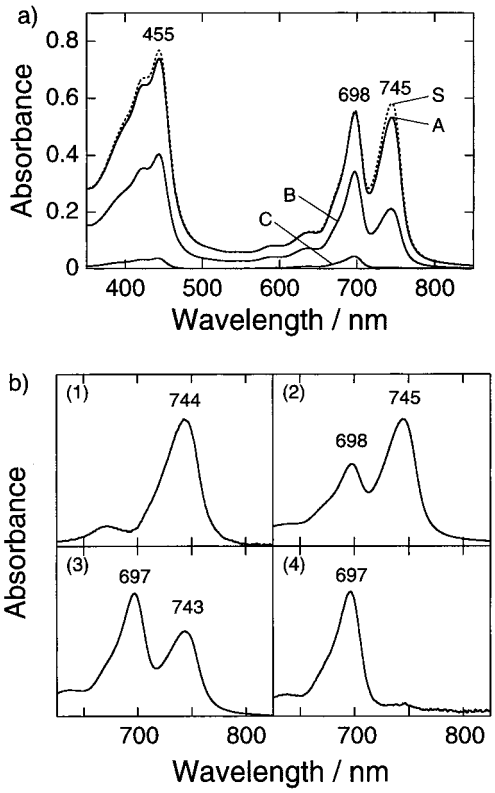

Figure 6. (a) Visible absorption spectra of filtrate of the aggregate solution ($x_A = 0.49$, 2P 26%, 10 μM on monomer basis, 25 °C). Dotted curve S, before filtration; solid curves A, B, and C, filtrates by filter A, B, and C (pore sizes, A > B > C; see text). (b) Visible absorption spectra of the colloidal fraction of different particles sizes. Spectrum 1, largest colloidal size fraction (=curve S − curve A); spectrum 2, second largest fraction (=curve A − curve B); spectrum 3, second smallest fraction (=curve B − curve C); spectrum 4, smallest fraction (=curve C).

a decrease in the colloidal size was concurrent with a decrease of the 745 nm band, an increase of the 698 nm band, and a decrease of x_A (content of Chl *a*) of the particle. An aggregate solution of an epimeric mixture of $x_A = 0.49$ (an average particle size, ca. 210 nm) which gave a typical double-peaked Q_y absorption (dotted curve S in Figure 6a) was loaded on filters A, B, and C (pore size: A > B > C), and three different filtrates were obtained. DLS measurements revealed that sizes of colloids in these filtrates were less than ca. 300 nm (filter A), ca. 210 nm (filter B), and ca. 150 nm (filter C), respectively (cf. average hydrodynamic diameters of the pure Chl *a* and *a*′ aggregates, ca. 500 nm and ca. 120 nm, respectively). Solid curves A−C in Figure 6a show absorption spectra of these filtrates. Most of the colloidal particles passed through filter A, as demonstrated by little change in the absorption spectrum, the average particle size (ca. 180 nm), and the epimeric composition ($x_A = 0.49$) of the filtrate (solid curve A in Figure 6a). Filter B fractionated larger amount of colloids than filter A; the 745 nm band diminished to a greater extent than the 698 nm one (curve B), and the epimeric composition decreased from 0.49 to 0.37. Only a small part of the colloids could escape from filter C; this filtration drastically reduced an epimeric composition (0.49 → 0.26) and gave a single Q_y absorption band at 698 nm and a Soret peak at 443 nm (curve C).

Figure 6b illustrates spectra of colloidal fractions of different particle sizes, obtained by the subtraction between the spectra in Figure 6a. The largest class of colloidal particles yielded a spectrum characteristic of the Chl *a*-type aggregate: a broad Q_y band at 744 nm and a Soret peak at 449 nm (spectrum 1 in

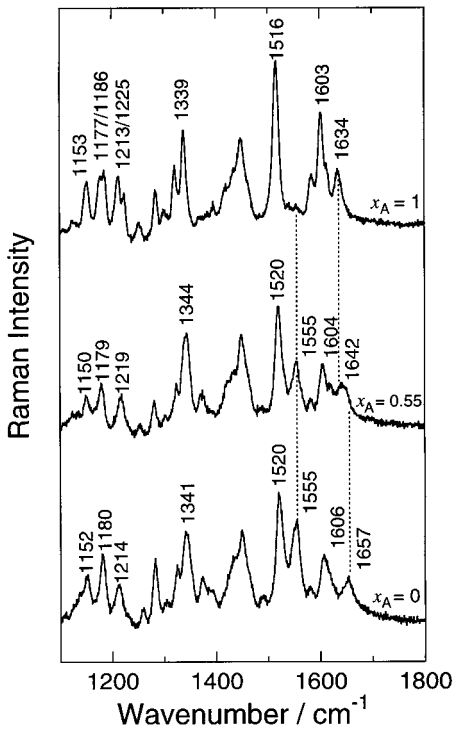

Figure 7. Resonance Raman spectra of Chl *a*/*a*′ aggregates formed in 2P 26% (50 μM on monomer basis, 25 °C). Top, pure Chl *a* aggregate ($x_A = 1$); middle, the Chl *a*/*a*′ mixed aggregate ($x_A = 0.55$); bottom, pure Chl *a*′ aggregate ($x_A = 0$).

Figure 6b, =curve S − curve A; cf. the top curve in Figure 2). The second largest fraction of the colloids gave a small 698 nm band in the blue side of the 745 nm band (curve 2, curve A − curve B). The 698 nm band became more intense than the 745 nm one in the spectrum of the second smallest colloidal fraction (curve 3, curve B − curve C). Then, the smallest part showed the 698 nm band nearly exclusively in the Q_y region, as in the spectrum of the Chl *a*′-type aggregate (curve 4, = curve C; cf. the bottom curve in Figure 2).

Resonance Raman and Circular Dichroism Spectra. RR and CD spectra suggest that most of the Chl *a* and *a*′ aggregate structures did not form separate colloids. Figure 7 depicts RR spectra of the aggregates formed at $x_A = 1$, 0.55, and 0 (λ_{ex} = 457.9 nm). The RR spectra of the pure Chl *a* ($x_A = 1$) and the pure Chl *a*′ aggregates ($x_A = 0$) are clearly distinguished from each other by remarkable differences in, e.g., the position of the C13^1-keto stretching bands (Chl *a*, 1634 cm^{-1}; Chl *a*′, 1657 cm^{-1}) and the presence (Chl *a*′) or absence (Chl *a*) of the skeletal C═C vibrational band at 1555 cm^{-1}.[12,24,25,31,32] The RR spectrum of the Chl *a*/*a*′ mixture aggregate of $x_A = 0.55$ (middle in Figure 7) gives a C═C vibrational band at 1555 cm^{-1} whose intensity (relative to the ∼1520 cm^{-1} peak) is less than that of the pure Chl *a*′ aggregate. The C13^1-keto stretching band spreads over a wide range of 1630−1660 cm^{-1} covering the keto band positions characteristic of the pure Chl *a* and *a*′ aggregates. It is noted, however, that a simple weighed sum of the RR spectra of the pure Chl *a* and *a*′ aggregates did not fully fit the observed spectra of the mixed aggregates (data not shown).

The CD spectrum of the epimeric mixture aggregate (x_A = 0.55) also cannot be reproduced by a linear combination of the CD spectra of the pure Chl *a* and *a*′ aggregates (Figure 8). The pure Chl *a* aggregate ($x_A = 1$) gives an intense, broad, negative CD component peaking at 757 nm and a minor positive peak at around 715 nm (dotted curve). The pure Chl *a*′ aggregate ($x_A = 0$) gives a dispersed-type CD couplet whose positive and negative lobes are located at 694 and 706 nm, respectively (broken curve); the shape of this spectrum is reminiscent of that of the Chl *a*′ aggregate formed in aqueous methanol,[12,24] suggesting a similarity in the aggregate structure. The CD spectrum of the aggregate of $x_A = 0.55$ also shows a dispersed-type feature (solid curve). The positive and negative peaks are at 742 and 765 nm, respectively, which are different from the peak positions of the Chl *a* aggregate and the Chl *a*′ aggregate. The spectrum is more intense, more distorted, and much more broadened than that of the Chl *a*′ aggregate.

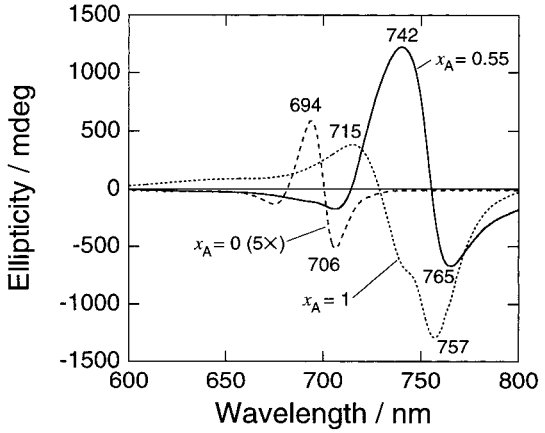

Figure 8. CD spectra of Chl *a*/*a*′ aggregates formed in 2P 26% obtained under the similar conditions as in Figure 2 (10 μM on monomer basis, 25 °C). Solid curve, Chl *a*/*a*′ mixed aggregate (x_A = 0.55); broken curve, pure Chl *a*′ aggregate ($x_A = 0$); dotted curve, pure Chl *a* aggregate ($x_A = 1$).

Discussion

Spontaneous Separation between Chl *a* and *a*′. The aggregation of the Chl *a*/*a*′ epimeric mixture of ca. 1:1 in aqueous 2-propanol afforded the two Q_y absorption bands at ∼745 and ∼698 nm where the pure Chl *a* and *a*′ aggregates gave their characteristic Q_y bands, respectively (Figure 2). The fluorescence excitation spectrum (Figure 3b) as well as the filtration experiments (Figure 6) clearly demonstrate that the 745 and 698 nm absorption bands originated from different aggregate structures coexisting in the solution. The finding of the systematic spectral change (Figure 6) with the change in the epimeric composition of the filtrates (x_A, 0.49 → 0.26) leads to the 698 nm and 745 nm absorption bands being assigned to the Chl *a*′-rich and Chl *a*-rich aggregate structures, respectively. This is supported by the finding that, in the early disaggregation stage, the 698 nm band decreased preferentially to enrich monomeric Chl *a*′ (Figure 5), in view that the Chl *a*′-rich aggregate colloids tended to be smaller particles and disappeared prior to the larger, Chl *a*-type aggregate colloids (Figure 6). The assignment is also in line with the concurrent decrease of size and x_A of the aggregate colloid, because the colloidal particles of the pure Chl *a* aggregate were larger than those of the pure Chl *a*′ aggregate. Thus, it can be said that Chl *a* and *a*′ tended to form the separate self-aggregates spontaneously.[33]

Fluorescence emission, RR, and CD spectroscopies revealed the difference between the aggregate colloid of Chl *a*/*a*′ (=ca. 1/1) epimeric mixture and the colloidal mixture of the pure Chl *a* and *a*′ aggregates (Figures 3, 7, and 8). The inconsistency suggests that two types of the aggregate structures coexisted mostly in each colloidal particle. Because the aggregates of the ordered structures developed more slowly than the enhancement of the colloidal particles (Figure 4), the binary colloidal particles may be formed by separation of the Chl *a* and *a*′ during

transformation from the amorphous structure into the ordered structures in each particle, rather than by coalescence of the mature Chl *a*-type and Chl *a*′-type aggregate colloids. A small amount of the unexpected epimer was involved in the lattice of the growing aggregate structures. It is assumed that less than 30% of the Chl *a*′ (Chl *a*) can be incorporated into the Chl *a* (Chl *a*′) aggregate domain, as judged from the epimeric compositions of the single-Q_y-peak/double-Q_y-peaks boundaries at x_A = ca. 0.3 and 0.7 (Figure 2).

Mechanism of the Aggregation. The above view is rationalized by invoking the following mechanism of aggregation. At the instant of water admixing to Chl in 2-propanol, Chl molecules abruptly associate together in a supercooled state to form amorphous aggregate colloids that give the broad 672 nm Q_y absorption (kinetic control stage).[12,24] These precursor colloids experience collision and coalescence through diffusion in the aqueous solution, resulting in enhancement of the colloidal size.[24] An increase of density (pressure) in the enhanced particle may induce reorganization of Chl molecules into more stable, densely packed structures (thermodynamic control stage).[12,25] Such a slow transformation (phase transition) in solid particles is demonstrated by the gradual development of the 698 and 745 nm bands at the expense of the broad 672 nm absorption (Figure 4).

In case of the epimeric mixture, the amorphous precursor aggregate has to contain both epimers, since the abrupt aggregation in the kinetic control stage occurs much more rapidly than molecular recognition, i.e., epimerical separation. The epimeric composition of *a particle* of the precursor aggregate can be expressed as a Gaussian distribution function peaking at an x_A of *the solution* (=an average x_A of all particles). Even after collision and coalescence, the epimeric composition of *a particle* should show a similar distribution. Then the particles can expereince the phase transition process as follows. (i) For a particle of x_A = 0.5−0.7 (0.3−0.5), the major component Chl *a* (*a*′) molecules in a particle gradually change their orientation with an increasing pressure and afford the ordered aggregate structure characteristic of Chl *a* (*a*′). Chl *a*′ (*a*) molecules, the other epimer, are squeezed out of the growing domains of the ordered structure of the Chl *a* (*a*′) aggregate containing a small amount of Chl *a*′ (*a*). The remaining amorphous part in the particle diminishes with enrichment of Chl *a*′ (*a*) and finally transforms into the ordered aggregate structures. (ii) For a particle of x_A = 0.7−1 (0−0.3), the process goes as (i) but does not leave enough Chl *a*′ (*a*) molecules giving no Chl *a*′ (*a*) aggregate domain, because all Chl *a*′ (*a*) molecules can be incorporated into the Chl *a* (*a*′) aggregate domains. Relative amounts of these four types of particles in the solution determine the total absorption spectrum.

The incorporation should result in partial structural defects which could distort the RR spectra (Figure 7) and broaden the 745 nm absorption band (Figures 2, 3b, 5, and 6b). The particles of x_A = 0.3−0.7 afford islands of two types (the Chl *a* and Chl *a*′ types) of the ordered aggregates scattered in a common colloidal particle; the CD spectrum of the epimeric mixture aggregate (Figure 8) may reflect the complicated three-dimensional distribution of the Chl *a* and *a*′ aggregate domains in the colloidal particle, in view of general observation that the CD spectrum depends strongly on a long-range chirality of the supramolecular architecture.[34] A part of Chl *a* may form an intermediate aggregate structure which gives a Q_y band at around 700 nm (Figure 4b).[24]

Theoretical Interpretation. The crucial process of this diastereoselective phenomenon can be regarded as a phase separation between the ordered aggregate domains of Chl *a* and *a*′ through the phase transition from the amorphous state to the ordered aggregates. It is noted that this process is essentially the same as the formation of a two-phase alloy or the separation of mutually similar organic liquids or gels with decreasing temperature of the mixture. These are rationalized in terms of the behavior of a regular solution, to a first approximation. The theoretical application requires the following assumptions for an epimeric pair of chlorophyllous pigments. (i) Two phases (two aggregate domains characteristic of respective epimers) are in equilibrium as postulated in the above aggregation mechanism. (ii) The two epimers can mix randomly; this was confirmed by the formation of the precursor amorphous aggregate. (iii) van der Waals forces dominate the intermolecular interactions in the aggregates; such may be the case for the aggregates of Chl derivatives which possess the C17-long aliphatic chains.[35]

Here, the free energy of the mixing of an epimeric pair of chlorophyllous pigments (ΔG) is written as

$$\Delta G/RT = x_A \ln x_A + x_B \ln x_B + K x_A x_B \quad (1)$$

$$K \propto [\sqrt{(\Delta E_{VA})} - \sqrt{(\Delta E_{VB})}]^2 \quad (1')$$

where x_A and x_B (=1 − x_A) are the mole fractions of the epimers, R is the gas constant, T is the temperature, and K denotes a parameter depending on the interactions between the epimers defined as a difference in the molar lattice energies per unit volume of the aggregates of the epimers (ΔE_{VA} and ΔE_{VB}). Each set of aggregates of epimeric pairs has its own K. Equation 1 is differentiated to give

$$\partial[\Delta G/RT]/\partial x_A = \ln[x_A/(1 - x_A)] + K(1 - 2x_A) \quad (2)$$

The epimeric mixture is separated into two phases, when the chemical potential (2) has a common value at two different epimeric compositions. The condition $\partial[\Delta G/RT]/\partial x_A = 0$ yields

$$K = -[1 - 2x_A]^{-1} \ln[x_A/(1 - x_A)] \quad (3)$$

Equation 3 gives the compositions of the two coexisting phases at a given K, that is, a phase diagram (Figure 9). The coexistence curve is symmetric and parabolic (solid curve in Figure 9), and the minimum of the curve is at x_A = 0.5 and K = 2. Inside the solid curve is the two-phase region; the system brings only a single phase at any x_A when $K < 2$, and the phase separation occurs only when $K > 2$. Figure 9 is also consistent with an expectation that the clearer phase separation should occur for larger differences between the two aggregate structures or for a larger K value. The broken line denotes spinodal compositions derived from the condition

$$\partial^2[\Delta G/RT]/\partial x_A{}^2 = 0 \quad (4)$$

The areas between the solid and broken lines in Figure 9 represent the metastable regions with respect to demixing. The epimeric composition dependence of the absorption spectrum (Figure 2) indicated the phase separation boundary of x_A = ca. 0.3 and 0.7. This leads to K = 2.1 for the present Chl *a*/*a*′ mixed system.

The above simple model qualitatively fits the observed phase behavior of the Chl *a*/*a*′ system; the phase separation occurred between certain boundary compositions of x_A' (=0.3) and x_A'' (=0.7). Thus, the unexpected epimer was incorporated in each separated phase, and below x_A' and above x_A'', the system gives

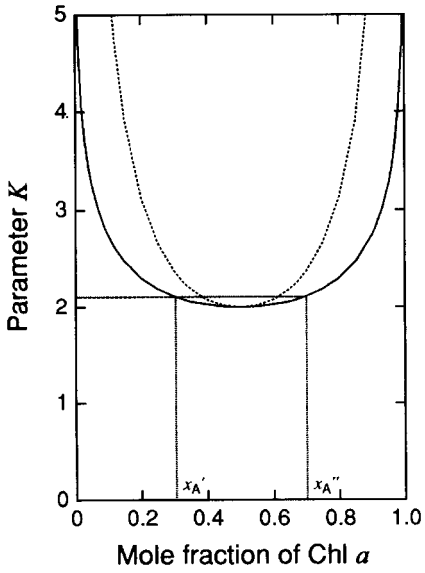

Figure 9. Phase diagram of the mixture aggregate of chlorophyllous pigments in terms of the interaction parameter K (see text). The solid curve represents the coexistence line, and the broken curve shows the spinodal line. Inside the solid curve is the two-phase region.

a single phase with an aggregate structure reflecting that of the major epimer. The consistency suggests the validity of the postulated aggregation mechanism and the assumptions for this theoretical interpretation. Essential similarity in the molecular structures of Chl *a* and *a*′ is responsible for the ideal behavior ($x_A' = 1 - x_A''$). The analysis also suggests that solvent molecules which might be incorporated into the aggregates did not affect the diastereoselective behavior. A complicated behavior observed for the Chl *a*/*a*′ system in methanol/water = 60:40[23] may come from much faster aggregations, which can bring the system into metastable states,[24] and from monitorings for only short time (within 30 min from the mixing).

Chlorosomal Chl Self-Aggregates. We can now speculate whether the C3[1]-epimers of chlorosomal Chls (BChls *c*, *d*, and *e*) form the self-aggregates diastereoselectively based on the theoretical interpretation described above. The oligomers of chlorosomal Chls are formed through intermolecular hydrogen bonding between the C3[1]-hydroxyl group and the C13[1]-keto carbonyl group and coordination interaction between the C3[1]-hydroxyl group and the central Mg atom. Because these intermolecular linkages are similar to the hydrogen bonding networks in the Chl *a* aggregate,[25,39,40] it is reasonable to suppose that van der Waals forces also contribute dominantly to the molecular interactions in the aggregates of chlorosomal Chls; the above theoretical study may also hold for the oligomerization of chlorosomal Chls in aqueous alcohols. It is noted that the aggregates of both C3[1]-(R) and -(S) epimers have essentially the same modes of intermolecular linkages (Mg···OH···O═C). The difference between the molar lattice energies of their aggregates (ΔE_{VA} and ΔE_{VB}) may be very small, if the stereochemistry of the C3[1]-methyl group gives little difference in the interactions between the macrocycles (the $\pi-\pi$ interaction and van der Waals interactions); the aggregates (micelles, gels, or liquid crystallines) of chlorosomal Chls may have a much smaller K value than that of the Chl *a*/*a*′ mixture (Figure 9). The facile ligation of the C3[1]-hydroxyl group to the metal atom makes the aggregation of chlorosomal Chls much faster than those of the Chl *a*/*a*′ mixture (A Chl derivative possessing a hydroxyl group formed the final form of the self-aggregate at the instant of preparation in the same medium of 2-propanol/water = 26:74.[41]), and probably much faster than the recognition of the C3[1]-chirality, which facilitates bringing the system into a supercooled state and inhibits phase separation. These strongly point to a possibility that chlorosomal Chls do not show the spontaneous, diastereoselective separation in the formation of micelles, gels, or liquid crystallines in vitro. This is consistent with such previous observations that a BChl *c* epimeric mixture of R/S = 2:1 showed an aggregation behavior quite similar to that of the pure R epimer.[20]

Because little is known about the mechanism of Chl self-aggregation in chlorosomes, we can make only much more limited comment on separation/mixing of the epimers of BChl *c* analogues in the in vivo aggregate. We speculate that the C3[1] epimers may also self-assemble randomly in vivo, if the aggregation occurs in essentially the same way as in the above in vitro system: (1) no specific process stores each C3[1]-epimer in the separate pool before the formation of the aggregates; (2) the aggregate is not formed by sequential polymerization[42] but by coalescence of small amorphous clusters followed by phase transition; (3) the aggregation is completed in at least 20 h; (4) each Chl aggregate has a large number of Chl molecules; (5) thus-formed aggregate structure does not experience any annealing processes.[42]

The present analysis suggests that the C17-long alkyl chain, and thus van der Waals interaction, plays a crucial role in the formation of the aggregate. This may also hold for the Chl aggregates in chlorosome. The interactions between the C17-long chains can determine the supramolecular structure, which may be closely correlated with the antenna function.[43] Further studies on the in vivo function of Chl *a*′ as well as the supramolecular structure of the chlorosomal Chl self-aggregates are now under way.

Acknowledgment. We are grateful to Dr. Z.-Y. Wang, Tohoku University, for valuable advice and discussions, to Mr. G. Katano, Institute of Industrial Science, University of Tokyo, and Dr. M. Mimuro, National Institute for Basic Biology (present address, Yamaguchi University), for their help in experiments, and to Dr. T. Miyatake, Ritsumeikan University, for discussions. We also thank Otsuka Electronics for giving us standard samples for DLS measurement.

References and Notes

(1) Ramanathan, N.; Currie, A. L.; Colvin, J. R. *Nature* **1961**, *190*, 779−781.
(2) Tachibana, T.; Kambara, H. *J. Am. Chem. Soc.* **1965**, *87*, 3015−3016.
(3) Nakashima, N.; Asakuma, S.; Kunitake, T. *J. Am. Chem. Soc.* **1985**, *107*, 509−510.
(4) Fuhrhop, J. H.; Boettcher, C. *J. Am. Chem. Soc.* **1990**, *112*, 1768−1776.
(5) Gulik-Krzywicki, T.; Fouquey, C.; Lehn, J. M. *Proc. Natl. Acad. Sci. U.S.A.* **1993**, *90*, 163−167.
(6) Ushio, T.; Tamura, R.; Takahashi, H.; Azuma, N.; Yamamoto, K. *Angew. Chem., Int. Ed. Engl.* **1996**, *35*, 2372−2374.
(7) Blankenship, R. E.; Olson, J. M.; Miller, M. In *Anoxygenic photosynthetic bacteria*; Blankenship, R. E., Madigan, M. T., Bauer, C. E., Ed.; Kluwer Academic Publishers: Dordrecht, The Netherlands, 1995; Chapter 20, pp 401−435.
(8) Olson, J. M. *Photochem. Photobiol.* **1998**, *67*, 61−75.
(9) Tamiaki, H. *Coord. Chem. Rev.* **1996**, *148*, 183−197.
(10) Maeda, H.; Watanabe, T.; Kobayashi, M.; Ikegami, I. *Biochim. Biophys. Acta* **1992**, *1099*, 74−80.
(11) Nakamura, A.; Watanabe, T. *FEBS Lett.* **1998**, *426*, 201−204.
(12) Oba, T.; Watanabe, T.; Mimuro, M.; Kobayashi, M.; Yoshida, S. *Photochem. Photobiol.* **1996**, *63*, 639−648.
(13) Fages, F.; Griebenow, N.; Griebenow, K.; Holzwarth, A. R.; Scaffner, K. *J. Chem. Soc., Perkin Trans. 1* **1990**, 2791−2797.
(14) Smith, K. M.; Craig, G. W.; Kehres, L. A.; Pfennig, N. *J. Chromatogr.* **1983**, *281*, 209−223.
(15) Smith, K. M.; Goff, D. A. *J. Chem. Soc., Perkin Trans. 1* **1985**, 1099−1113.

(16) Simpson, D. J.; Smith, K. M. *J. Am. Chem. Soc.* **1988**, *110*, 1753−1758.
(17) Uehara, K.; Olson, J. M. *Photosynth. Res.* **1992**, *33*, 251−257.
(18) Tamiaki, H.; Takeuchi, S.; Tanikaga, R.; Balaban, T. S.; Holzwarth, A. R.; Scaffner, K. *Chem. Lett.* **1994**, 401−402.
(19) Balaban, T. S.; Holzwarth, A. R.; Scaffner, K. *J. Mol. Struct.* **1995**, *349*, 183−186.
(20) Chiefari, J.; Griebenow, K.; Griebenow, N.; Balaban, T. S.; Holzwarth, A. R.; Schaffner, K. *J. Phys. Chem.* **1995**, *99*, 1357−1365.
(21) Balaban, T. S.; Tamiaki, H.; Holzwarth, A. R.; Schaffner, K. *J. Phys. Chem. B* **1997**, *101*, 3424−3431.
(22) Tamiaki, H.; Takeuchi, S.; Tsuzuki, S.; Miyatake, T.; Tanikaga, R. *Tetrahedron* **1998**, *54*, 6699−6718.
(23) Watanabe, T.; Kobayashi, M.; Hongu, A.; Oba, T. *Chem. Lett.* **1992**, 1847−1850.
(24) Oba, T.; Mimuro, M.; Wang, Z.-Y.; Nozawa, T.; Yoshida, S.; Watanabe, T. *J. Phys. Chem. B* **1997**, *101*, 3261−3268.
(25) Oba, T.; Furukawa, Wang, Z.-Y.; Nozawa, T.; H.; Mimuro, M.; Tamiaki, H.; T.; Watanabe, T. *J. Phys. Chem. B* **1998**, *102*, 7882−7889.
(26) Hynninen, P. H.; Lötjönen, S. *Synthesis* **1983**, 705−708.
(27) Watanabe, T.; Hongu, A.; Honda, K.; Nakazato, M.; Konno, M.; Saitoh, S. *Anal. Chem.* **1984**, *56*, 251−256.
(28) Oba, T.; Kobayashi, M.; Yoshida, S.; Watanabe, T. *Anal. Sci.* **1996**, *12*, 281−284.
(29) The Q_y band of the pure Chl *a* aggregate was observed in the excitation spectrum situated at around 735 nm, which was ca. 10 nm shorter than that in the absorption spectrum. This may be caused by scattering or reflection from the colloidal particles.[24,30]
(30) Jacobs, E. E.; Holt, A. S.; Kromhout, R.; Rabinowitch, E. *Arch. Biochem. Biophys.* **1957**, *72*, 495−511.
(31) Fujiwara, M.; Tasumi, M. *J. Phys. Chem.* **1986**, *90*, 250−253.
(32) Boldt, N. J.; Donohoe, R. J.; Birge, R. R.; Bocian, D. F. *J. Am. Chem. Soc.* **1987**, *109*, 2284−2298.
(33) Though we cannot fully exclude the possibility of the formation of $C13^2$-epimerically mixed compounds (Chl *a*/*a*′ "hetero" aggregates), we think that it is negligible; the epimers should inherently be separated, because Chl *a* and *a*′ are diastereomers and the properties of the epimers are different. We suppose that Chl *a* and *a*′ molecules that were not introduced into the Chl *a* and *a*′-type aggregate structures remained as the amorphous, precursor aggregates seen as shoulder components of the Q_y bands (at around 670 nm, Figure 2).
(34) Kim, M.-H.; Ulibarri, L.; Keller, D. *J. Chem. Phys.* **1986**, *84*, 2981−2989.
(35) van der Waals interactions between the C17-phytyl ($C_{20}H_{39}$) chains in the aggregates are expected to be larger than the molar lattice energy of crystalline octadecane ($C_{18}H_{38}$, 126 kJ mol^{-1}).[36] The interactions between two zinc−porphyrin macrocycles, probably similar to those between the chlorin macrocycles, were estimated to be ca. 50−60 kJ mol^{-1}, originating mostly in the van der Waals interactions which were much stronger than the $\pi-\pi$ interaction.[37] Thus, the total van der Waals interactions between Chl molecules may be much larger than the possible hydrogen bondings and coordination interactions between the peripheral substituents or additional water molecules and the central Mg atom, as judged from amino acid/zinc−porphyrin interactions (ca. 50−60 kJ mol^{-1}).[38]
(36) Israelachvili, J. N. In *Intermolecular and Surface Forces*; Academic Press: London, 1985; Chapter 6.2, p 71.
(37) Hunter, C. A.; Sanders, J. K. M. *J. Am. Chem. Soc.* **1990**, *112*, 5525−5534.
(38) Ogoshi, H.; Mizutani, T. *Acc. Chem. Res.* **1998**, *31*, 81−89.
(39) Chow, H.; Serlin, R.; Strouse, C. E. *J. Am. Chem. Soc.* **1975**, *97*, 7230−7237.
(40) Kratky, C.; Dunitz, J. D. *J. Mol. Biol.* **1977**, *113*, 431−442.
(41) Oba, T.; Tamiaki, H. *Photochem. Photobiol.* **1998**, *67*, 295−303.
(42) It may be assumed that (1) BChl molecules self-assemble successively inside the chlorosomes after slow transfer of each Chl molecule into the chlorosomal lipid from the cytoplasm and (2) thus-formed in vivo aggregate structure is rigid sufficiently; these processes should provide the epimerically separated self-aggregates.
(43) Buck, D. R.; Struve, W. S. *Photosynth. Res.* **1996**, *48*, 367−377.